Luminescence and charge carrier trapping in YPO_4:Bi

Awater, Roy; Niemeijer-Berghuijs, Louise C.; Dorenbos, Pieter

DOI
10.1016/j.optmat.2017.02.032

Publication date
2017

Document Version
Final published version

Published in
Optical Materials

Optical Materials 66 (2017) 351–355

Contents lists available at ScienceDirect

Optical Materials

journal homepage: www.elsevier.com/locate/optmat

Luminescence and charge carrier trapping in YPO_4:Bi

Roy H.P. Awater*, Louise C. Niemeijer-Berghuijs, Pieter Dorenbos

Luminescence Materials Research Group (FAME-LMR), Department of Radiation Science and Technology, Faculty of Applied Sciences, Delft University of Technology, 2629 JB, Delft, The Netherlands

ARTICLE INFO

Article history:
Received 14 February 2017
Received in revised form
16 February 2017
Accepted 16 February 2017

Keywords:
Bi^{2+}
Bi^{3+}
Bi-pairs
YPO_4
Electron trap
Hole trap

ABSTRACT

YPO_4 doped with Bi^{3+} and/or Tb^{3+} samples were prepared in air. X-ray excited luminescence measurements showed emission from isolated Bi^{3+} and Bi-pairs, and also emission from Bi^{2+} was observed. Based on the obtained spectroscopic data, the electron binding energies in the ground and excited states of Bi^{3+} and Bi^{2+} were placed inside the vacuum referred binding energy (VRBE) scheme, and this was used to explain the luminescence of bismuth doped YPO_4. The VRBE scheme and additional thermoluminescence glow curves show that bismuth can act both as electron and as hole trap in YPO_4.

1. Introduction

Bi^{3+} is a well-studied activator and sensitizer for luminescent materials [1]. The Bi^{3+} ion has the $6s^2$ outer electron configuration, and optical transitions to three 6s6p excited states, labeled as A-, B- and C-bands, can be observed. Also a metal-to-metal charge transfer (MMCT) from the Bi^{3+} ground state to the host conduction band (CB) is commonly observed. In addition to the characteristic A-band emission, a lower energy emission band is frequently reported [2]. There is still controversy about the origin of this lower energy emission band. In a recent evaluation, Boutinaud tentatively assigned it to CB→ Bi^{3+}/Bi^{4+} CT luminescence [3]. Alternatively, Srivastava assigned the additional emission band in $Y_2Sn_2O_7$ and $GdAlO_3$ to emission from Bi^{3+}–Bi^{3+} pairs or clusters [4,5]. Also Wolfert et al. proposed in the 1980s that bismuth pairs can be the origin of the additional emission observed in Bi^{3+}-doped rare earth borates and oxychlorides [6,7].

In 1994, Blasse et al. confirmed the luminescence of the unique divalent bismuth oxidation state in SrB_4O_7 and $BaSO_4$ [8,9]. Later, Bi^{2+} luminescence was also reported in alkaline-earth fluorides, sulfates, phosphates and borates for white-light LED applications [10–14] Divalent bismuth shows luminescence in the orange-red to infrared part of the spectrum. With excitation bands in the near ultraviolet (NUV) and blue, Bi^{2+}-doped phosphors are ideal to be used in combination with an InGaN LED in order to make white light LEDs [15]. Furthermore, the red radioluminescence reported for $Sr_2P_2O_7$:Bi^{2+} spectrally matches with the sensitivity of silicon-based semiconductor detectors, making Bi^{2+} a promising activator ion for the next generation long wavelength emitting scintillator materials [16]. The difficulty is to stabilize Bi^{2+} in the host lattice. Usually, a reducing atmosphere is required. Peng et al. showed that Bi^{2+} can also be stabilized in over-stoichiometric barium phosphates [17]. Recently, we reported that X-ray induced reduction of Bi^{3+} to Bi^{2+} is possible in $Li_2BaP_2O_7$:Bi [18]. In this work we show divalent bismuth radioluminescence from bismuth ions doped on trivalent host lattice sites.

In order to gain more insight in the trapping and luminescence properties of bismuth, we selected YPO_4:Bi as our compound of interest. YPO_4 is a wide band gap compound with only one crystallographic Y-site where Bi^{3+} can be situated. Its electronic structure is well-established from lanthanide spectroscopy and also the spectroscopy of YPO_4:Bi has been discussed in literature [19–21]. In order to estimate the VRBE in the Bi^{2+} ground state in YPO_4, thermoluminescence measurements of co-doped YPO_4:Bi, Tb were performed. We discovered that bismuth acts as both electron and hole trap, and that in the case of YPO_4, the hole is trapped more shallower than the electron.

* Corresponding author.
E-mail address: R.H.P.Awater@tudelft.nl (R.H.P. Awater).

http://dx.doi.org/10.1016/j.optmat.2017.02.032
0925-3467/

2. Experimental

Samples of YPO_4 doped with varying amounts of Bi^{3+} and/or Tb^{3+} were prepared using conventional solid-state sintering. Stoichiometric amounts of the starting materials Y_2O_3 (99.99%), $(NH_4)H_2PO_4$ (99.999%), Bi_2O_3 (99.999%) and Tb_2O_3 (99.999%) were thoroughly ground in acetone. The ground powders were first sintered at 400 °C for 10 h in air. After an intermediate grinding step in acetone, the samples were sintered at 1400 °C for 4 h in air. X-ray diffraction was used to check the phase purity of the samples using a PANalytical XPert PRO X-ray Diffraction system with a Co K_α ($\lambda = 0.71073$ Å) X-ray tube. The recorded patterns were compared with a reference pattern from the Pearson's Crystal Database to identify the formed phase and possible impurities. The X-ray excited emission spectra were recorded using an X-ray tube with Cu anode operating at 60 kV and 25 mA. The emission of the samples was focused via a quartz window and a lens on the entrance slit of an ARC VM504 monochromator, dispersed, and recorded with a Hamamatsu R943-02 PMT. The recorded spectra were corrected for the monochromator transmission and the quantum efficiency of the PMT. Photoluminescence excitation and emission measurements were recorded using a Hamamatsu L1835 D_2 lamp in combination with an ARC VM502 monochromator. The emission light of the samples was dispersed with a Princeton Instruments Acton SP 2300 monochromator and detected by a PerkinElmer Photon Counting Module MP1993. Thermoluminescence spectra were recorded using a RISØ TL/OSL reader model DA-15 with a DA-20 controller using a heating rate of 5 K/s. The samples were irradiated for 2 h using a ^{60}Co Gamma Cell 220 source with a dose rate of 0.29 Gy/s and were transported to the TL setup in complete darkness to prevent photobleaching.

3. Results

The XRD patterns of YPO_4:1.0% Bi and a reference spectrum from Pearson's Crystal Database No#1828017 are shown in Fig. 1. The diffraction peaks of the sample match well with that of the reference and no impurity phases are observed.

The photoluminescence excitation and emission spectra of YPO_4:1%Bi sample are shown in Fig. 2. The excitation spectrum was recorded while monitoring the 242 nm A-band emission and the emission spectrum was recorded while exciting at the 227 nm A-band absorption. Both spectra were recorded at room temperature. The 122 nm band in the excitation spectrum is attributed to the formation of free electrons and holes, *i.e.* the energy difference E_{vc} between the top of the valence band and the bottom of the conduction band. The wavelength of the host exciton creation in YPO_4 is well-established at 145 nm from lanthanide spectroscopy [22]. At

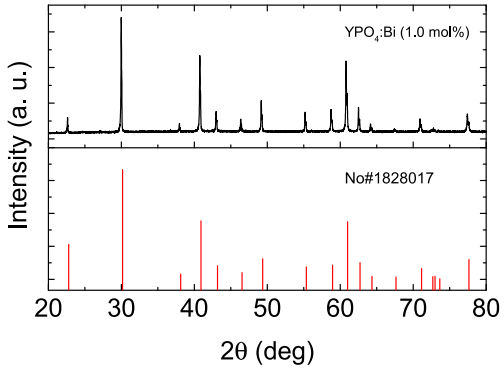

Fig. 1. XRD patterns of YPO_4:1.0% Bi and the reference No#1828017.

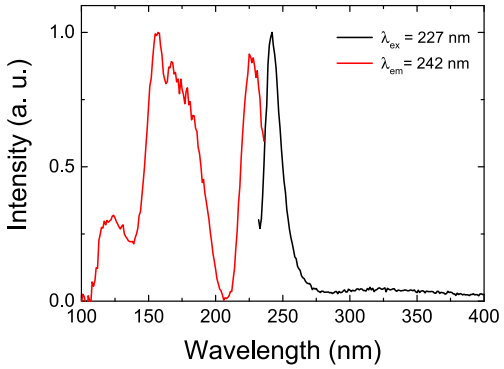

Fig. 2. Photoluminescence excitation (λ_{em} = 242 nm) and emission (λ_{ex} = 227 nm) spectra of YPO_4:1%Bi^{3+} measured at room temperature.

this wavelength a dip is observed in the excitation spectrum, indicating inefficient energy transfer from the exciton to Bi^{3+}. In the region between 150 and 200 nm excitation bands can be distinguished at 157 nm and 170 nm, which are attributed to the C-band excitation and $Bi^{3+} \rightarrow$ CB CT transitions, respectively. In the work by Cavalli et al. on YPO_4:Bi, only an unresolved broad band was reported in the region 150–200 nm [19]. The emission spectrum shows besides the 242 nm Bi^{3+} A-band emission a weak emission peaking at 325 nm. This emission has been attributed to Bi-pair emission by Srivastava et al., and they observed that the emission intensity increases with increasing Bi^{3+} concentration [21]. We observed no significant increase in the intensity of the Bi-pair emission band with varying the Bi^{3+} concentration between 0.05 and 2.0%.

The X-ray excited emission spectra of the Bi^{3+}-doped YPO_4 at room temperature are shown in Fig. 3. Undoped YPO_4 shows no radioluminescence in the measured region of 200 nm–800 nm. The bismuth-doped samples show the A-band emission at 242 nm, as well as additional emission bands at 300–550 nm and 670 nm. The A-band emission is most intense for a Bi^{3+} concentration of 0.05 mol% and decreases in intensity with increasing concentration of Bi^{3+}. Srivastava et al. observed a similar concentration dependence of the A-band emission in photoluminescence measurements [21]. The emission band observed at 670 nm has not been reported before for YPO_4. We attribute it to the $^2P_{3/2} \rightarrow {}^2P_{1/2}$ transition of Bi^{2+} caused by the trapping of an electron from the conduction band by Bi^{3+} to populate the excited Bi^{2+} state. Also the Bi^{2+} luminescence is most intense for the lowest concentration of 0.05% bismuth and decreases with increasing concentration. The

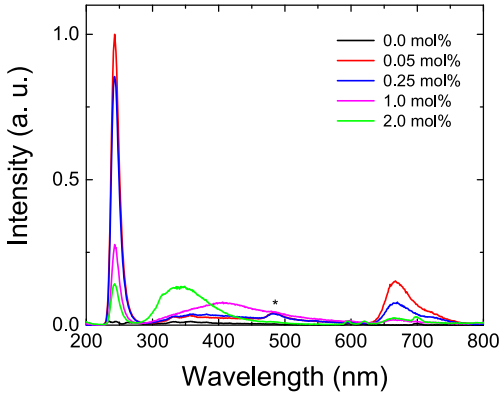

Fig. 3. X-ray excited emission spectra of YPO_4:Bi_X (x = 0.0, 0.05, 0.25 and 1.0 mol%) measured at room temperature. The asterisk at 480 nm marks the grating's second order reflection of the 242 A-band emission.

broad 300–550 nm emission band centered at 405 nm is probably due to electron hole recombination near an unknown defect, *i.e.* a near defect exciton (NDE) emission. A similar NDE emission band was observed by Bos et al. in $YPO_4:Tb^{3+}$ [23]. The intensity of the NDE emission band increases with increasing Bi^{3+} concentration. For a concentration of 2% bismuth, the NDE emission band has disappeared and a new band at 340 nm appears. This new band is the same as the pair emission observed in the photoluminescence spectra in Fig. 2.

Fig. 4 shows the temperature dependence of the A-band, pair-, Bi^{2+} and NDE emission under X-ray excitation for the sample with the lowest Bi concentration (0.05% Bi). The A-band gradually increases about 10% in intensity from 85 K up to 250 K. Then, the intensity increases rapidly to approximately 80% at 350 K and reaching 100% at 450 K, after which the intensity decreases again to 50% at 600 K. At temperatures below 170 K, NDE emission dominated the pair emission band. It disappears above 170 K and the Bi-pair emission starts to dominate. At the same temperature the Bi^{2+} emission appears and grows until reaching maximum intensity at 300 K. Above 300 K, the Bi^{2+} emission decreases until it is absent at 450 K.

Fig. 5 compares the X-ray excited emission spectra for YPO_4:1% Tb^{3+} and YPO_4:1%Tb^{3+}, 1%Bi^{3+} at room temperature. The bands labeled 1 and 2 originate from the Bi^{3+} A-band and NDE emission, respectively. The bands labeled 3–14 originate from Tb^{3+} 4f–4f transitions. Compared to the YPO_4:1%Tb^{3+} sample, the YPO_4:1% Tb^{3+}, 1%Bi^{3+} shows an increased intensity of the $^5D_4^7 \rightarrow F_{6-0}$ transitions (peaks nr. 8–14), while the $^5D_3^7 \rightarrow F_{6-2}$ transitions (peaks nr. 3–7) have slightly lower or the same intensity.

The thermoluminescence (TL) emission spectra of YPO_4:1%Tb^{3+} and YPO_4:1%Tb^{3+}, 1%Bi^{3+} are shown in Fig. 6. The TL glow peak of the YPO_4:1%Bi^{3+} sample is located at 425 K and shows Bi^{3+} A-band emission and a weak and broad emission at around 400 nm originating from mainly NDE emission. The TL glow peaks of the YPO_4:1%Tb^{3+},1%Bi^{3+} sample are observed at 425 K and 485 K with a shoulder glow on the higher temperature side, and it shows Bi^{3+} A-band emission, Tb^{3+} 4f-4f emission and weak broad band emission between 280 and 380 nm which is due to Bi-pair emission. No Bi^{2+} emission is observed during the TL measurements for both samples. The TL emission spectra of undoped YPO_4 and YPO_4:1%Tb^{3+} showed no thermoluminescence emission.

4. Discussion

Fig. 7 shows the vacuum referred binding energy (VRBE) scheme for YPO_4:Bi,Tb. The VRBE of the electron at the conduction band

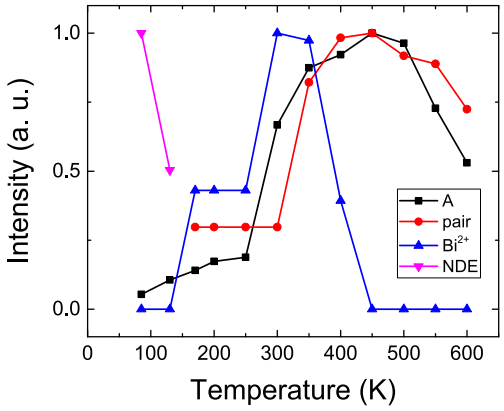

Fig. 4. Temperature dependence of the A-, pair-, Bi^{2+}-, and NDE emission bands derived from X-ray excited luminescence measurements of YPO_4:0.05%Bi. The intensity at the emission maximum is shown normalized to unity for each band.

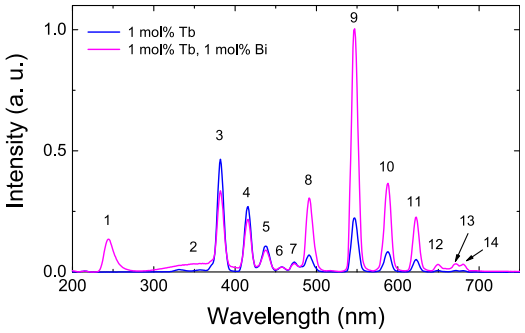

Fig. 5. X-ray excited emission spectra of YPO_4:1%Tb^{3+} and YPO_4:1%Bi^{3+},1%Tb^{3+} measured at room temperature.

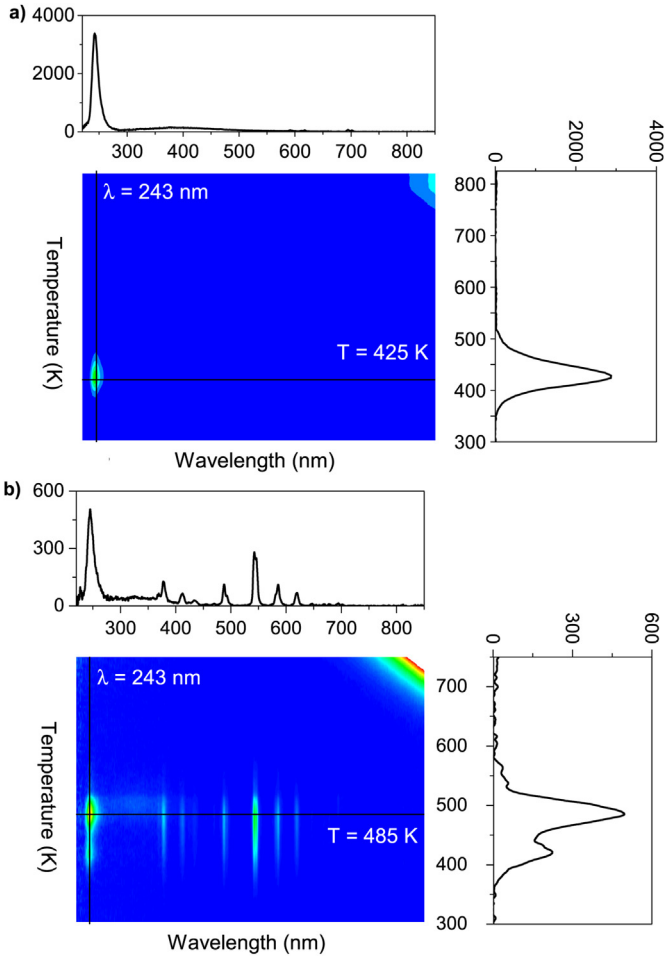

Fig. 6. TL emission spectrum of a) YPO_4:1.0% Bi and b) YPO_4:1.0% Bi, 1.0% Tb recorded after γ-ray irradiation for 2 h using a ^{60}Co source.

bottom ($E_C = -0.53$ eV), the valence band top ($E_V = -9.77$ eV), in the exciton state ($E^X = -1.22$ eV), and in the Tb^{3+} ground and excited states are taken from Ref. [24]. In order to estimate the VRBE in the $6s^2$ ground state of Bi^{3+}, the $Bi^{3+} \rightarrow$CB CT energy has been used. Similar to the interpretation of the Pr^{3+} and $Tb^{3+} \rightarrow$CB CT-energies in Ref. [25], we regard this energy (see arrow 1) as the energy difference between the Bi^{3+} ground state and $\frac{E_C+E_X}{2}$. One obtains −8.2 eV for the VRBE in the Bi^{3+} ground state, and by adding the 5.5 eV A-band energy (see arrow 2), −2.7 eV for the VRBE in the $^3P_1$ excited state.

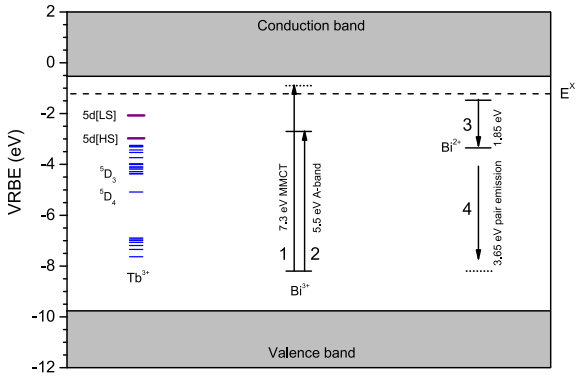

Fig. 7. Vacuum referred binding energy scheme of YPO_4 including the Tb^{3+}, Bi^{3+} and Bi^{2+} energy levels.

The X-ray excited emission spectra of YPO_4:Bi in Fig. 3 shows Bi^{2+} emission which is only possible when the $^2P_{3/2}(1)$ excited state is located well below the conduction band. Fig. 4 shows that the Bi^{2+} emission starts to quench at 350 K. With a typical radiative life time of 20 μs for Bi^{2+} emission [10,14] one may derive, with methods similar as in Ref. [26], the quenching energy barrier $\Delta E_q \approx T_{0.9}/620$ eV. Where $T_{0.9}$ is the temperature where the intensity has dropped by 10%. It corresponds more or less with the onset of thermal quenching. For quenching, the electron does not need to go fully to the conduction band and we will assume that $\frac{E_C+E_X}{2} - \Delta E_q$ provides a fair estimate for the VRBE in the Bi^{2+} excited state. The VRBE in the $^2P_{3/2}(1)$ excited state is then at −1.43 eV in Fig. 7 and using the emission energy of 1.85 eV (670 nm) (see arrow 3), the VRBE in the $^2P_{1/2}$ ground state is at −3.3 eV.

Upon X-ray irradiation, conduction band electrons can be captured by Bi^{3+} to first populate the excited state of Bi^{2+}, which is then followed by red luminescence of the $^2P_{3/2}(1) \rightarrow {}^2P_{1/2}$ transition (see arrow 3). Bi^{2+} is not stable in YPO_4 and will eventually recombine with a hole from the valence band or disappear by electron transfer to neighboring defects. Therefore, no Bi^{2+} related luminescence is observed under photon excitation.

The X-ray excited luminescence spectrum of YPO_4:Bi, Tb in Fig. 5 shows enhanced emission intensity from the Tb^{3+} $^5D_4 \rightarrow {}^7F_{7\text{-}0}$ transitions as compared to that of single-doped YPO_4:Tb. In single doped YPO_4:Tb^{3+}, the Tb^{3+} ions can be excited by first trapping a hole and later an electron, or by means of e-h pair capture, or energy transfer from the exciton or NDE state. In the presence of Bi^{3+} even more excitation paths are envisaged. Angiuli et al. already showed that $Bi^{3+} \rightarrow Tb^{3+}$ energy transfer occurs in YPO_4:Bi, Tb [27]. Probably also Tb^{4+}-Bi^{2+} pairs can be formed during X-ray exposure, and electron back transfer from Bi^{2+} may then also generate Tb^{3+} emission. Possibly, the electron transfer from Bi to Tb is more likely to populate the $^5D_4$ level.

In the TL emission spectrum of YPO_4:1%Bi in Fig. 6, a single glow peak is observed at 425 K which shows Bi^{3+} A-band emission at 243 nm. This indicates that the luminescence occurs from either electron capture on Bi^{4+} or from hole capture on Bi^{2+}. According to Fig. 7, Bi^{3+} can act as a 1.57 eV deep hole trap to form Bi^{4+} but also as a 2.97 eV deep electron trap to form Bi^{2+}. The hole will be released earlier from its trap than the electron. Besides the $Bi^{2+/3+}$ electron trap, other unknown host related electron traps may be present. Electron release from these unknown defects would generate besides Bi^{3+} emission (recombination on Bi^{4+}) also Bi^{2+} emission (recombination on Bi^{3+}). Since no Bi^{2+} emission is observed, the Bi^{3+} emission of the 425 K glow is attributed to Bi^{4+} hole release that recombines with Bi^{2+}. Supporting evidence is the absence of any thermoluminescence glow for YPO_4:Tb^{3+}. Tb^{3+} can only capture holes to form Tb^{4+} and only liberated electrons can recombine at Tb^{4+}. The formation of Bi^{4+} may seem strange since it is regarded as chemically unstable. Indeed during synthesis Bi^{4+} is never formed, however, since the Bi^{3+} ground state is above the valence band it can trap a hole to form Bi^{4+} as a meta-stable defect.

The TL emission spectrum of YPO_4:Bi, Tb in Fig. 6 shows both Bi^{3+} A-band and Tb^{3+} 4f-4f glow at 425 K and 485 K. We attribute the observed Tb^{3+} glow at 425 K to hole release from Bi^{4+} and recombination on Bi^{2+} followed by $Bi^{3+} \rightarrow Tb^{3+}$ energy transfer. In the VRBE scheme Tb^{3+} is predicted to act as a 2.1 eV deep hole trap which is 0.5 eV deeper than that by Bi^{3+}. We therefore attribute the 485 K glow peak to hole release from Tb^{4+}, which recombines with the Bi^{2+} electron trap, producing Bi^{3+} A-band glow and Tb^{3+} glow via energy transfer. Also weak Bi–Bi pair emission near 320 nm is visible at 485 K. Apparently, once the hole on Tb^{4+} is released it can migrate towards an electron trapped in a Bi–Bi pair resulting in the 3.65 eV pair emission. The rather low probability of this recombination mechanism accounts for its weak intensity. In the case of YPO_4:Bi, the pair emission is probably dominated by the NDE emission observed at around 400 nm.

5. Conclusions

X-ray excited emission spectra of YPO_4:Bi samples showed luminescence originating from Bi^{3+}, Bi^{2+} and Bi-pair emission. This work showed that characteristic red radioluminescence of Bi^{2+} is observed in YPO_4 doped with Bi^{3+}. Such type of radioluminecence may be utilized as red emitting scintillator material. The spectroscopic data on Bi^{3+} and Bi^{2+} was used to determine the VRBE of the electron in the ground and excited states of the Bi^{2+} and Bi^{3+}. The VRBE scheme, together with data from thermoluminescence glow curves showed that Bi^{3+} can act as both electron and hole trap in YPO_4.

Acknowledgments

This work was supported by the Dutch Technology Foundation STW, which is part of the Netherlands Organisation for Scientific Research, and which is partly funded by the Ministry of Economic Affairs. This work was partly funded by Saint Gobain Crystals, France.

References

[1] G. Blasse, A. Bril, Investigations of Bi^{3+}-activated phosphors, J. Chem. Phys. 48 (1968) 217–222.
[2] R.H.P. Awater, P. Dorenbos, The Bi^{3+} 6s and 6p electron binding energies in relation to the chemical environment of inorganic compounds, J. Lumin 184 (2017) 221–231.
[3] P. Boutinaud, Revisiting the spectroscopy of the Bi^{3+} ion in oxide compounds, Inorg. Chem. 52 (2013) 6028–6038.
[4] A.M. Srivastava, On the luminescence of Bi^{3+} in the pyrochlore $Y_2Sn_2O_7$, Mater. Res. Bull. 37 (2002) 745–751.
[5] A.M. Srivastava, H.A. Comanzo, The ultraviolet and visible luminescence of Bi^{3+} in the orthorhombic perovskite, $GdAlO_3$, Opt. Mater 63 (2017) 118–121.
[6] A. Wolfert, E.W.J.L. Oomen, G. Blasse, Host lattice dependence of the Bi^{3+} luminescence in orthoborates $LnBO_3$ (with Ln = Sc, Y, La, Gd or Lu), J. Solid State Chem. 59 (1985) 280–290.
[7] A. Wolfert, G. Blasse, Luminescence of the Bi^{3+} ion in compounds LnOCl (Ln = La, Y, Gd), Mater. Res. Bull. 19 (1984) 67–75.
[8] G. Blasse, A. Meijerink, M. Nomes, J. Zuidema, Unusual bismuth luminescence in strontium tetraborate (SrB_4O_7:Bi), J. Phys. Chem. Sol. 55 (1994) 171–174.
[9] M.A. Hamstra, H.F. Folkerts, G. Blasse, Red bismuth emission in alkaline-earth metal sulfates, J. Mater. Chem. 4 (1994) 1349–1350.
[10] R. Cao, F. Zhang, C. Liao, J. Qiu, Yellow-to-orange emission from Bi^{2+}-doped RF_2 (R = Ca and Sr) phosphors, Opt. Express 21 (2013) 15728–15733.
[11] R. Cao, M. Peng, J. Qiu, Photoluminescence of Bi^{2+}-doped $BaSO_4$ as a red phosphor for white LEDs, Opt. Express 20 (2012) A977–A983.
[12] M. Peng, L. Wondraczek, Photoluminescence of $Sr_2P_2O_7$:Bi^{2+} as a red phosphor for additive light generation, Opt. Lett. 35 (2010) 2544–2546.
[13] A.M. Srivastava, Luminescence of divalent bismuth in M^{2+} BPO_5 (M^{2+} = Ba^{2+},

Sr^{2+} and Ca^{2+}, J. Lumin. 78 (1998) 239–243.
[14] M. Peng, L. Wondraczek, Bi^{2+}-doped strontium borates for white-light emitting diodes, Opt. Lett. 34 (2009) 2885–2887.
[15] L. Li, M. Peng, B. Viana, J. Wang, B. Lei, Y. Liu, Q. Zhang, J. Qiu, Unusual concentration induced antithermal quenching of the Bi^{2+} emission from $Sr_2P_2O_7$:Bi^{2+}, Inorg. Chem. 54 (2015) 6028–6034.
[16] L. Li, B. Viana, T. Pauporté, M. Peng, Deep red radioluminescence from a divalent bismuth doped strontium pyrophosphate $Sr_2P_2O_7$:bi^{2+}, Proc. SPIE 9364 (2015), 936423 1–5.
[17] M. Peng, J. Lei, L. Li, L. Wondraczek, Q. Zhang, J. Qiu, Site-specific reduction of Bi^{3+} to Bi^{2+} in bismuth-doped over-stoichiometric barium phosphates, J. Mater. Chem. C 1 (2013) 5303–5308.
[18] R.H.P. Awater, P. Dorenbos, X-ray induced valence change and vacuum referred binding energies of Bi^{3+} and Bi^{2+} in $Li_2BaP_2O_7$, J. Phys. Chem. C 120 (2016) 15114–15118.
[19] E. Cavalli, F. Angiuli, F. Mezzadri, M. Trevisani, M. Bettinelli, P. Boutinaud, M.G. Brik, Tunable luminescence of Bi^{3+}-doped $YP_xV_{1-x}O_4$ ($0 \leq x \leq 1$), J. Phys. Condens. Matter 26 (2014) 385503.
[20] T. Jüstel, P. Huppertz, W. Mayr, D.U. Wiechert, Temperature-dependent spectra of YPO_4:Me (Me = Ce, Pr, Nd, Bi), J. Lumin 106 (2004) 225–233.
[21] A.M. Srivastava, S.J. Camardello, Concentration dependence of the Bi^{3+} luminescence in $LnPO_4$ (Ln = Y^{3+}, Lu^{3+}), Opt. Mater 39 (2015) 130–133.
[22] P. Dorenbos, A.J.J. Bos, N.R.J. Poolton, Carrier recombination processes and divalent lanthanide spectroscopy in YPO_4:Ce^{3+};L^{3+} L=Sm,Dy,Tm, Phys. Rev. B 82 (2010) 195127.
[23] A. Bos, P. Dorenbos, A. Bessiere, A. Lecointre, M. Bedu, M. Bettinelli, F. Piccinelli, Study of TL glow curves of YPO_4 double doped with lanthanide ions, Radiat. Meas. 46 (2011) 1410–1416.
[24] P. Dorenbos, The electronic level structure of lanthanide impurities in $REPO_4$, $REBO_3$, $REAlO_3$, and RE_2O_3 (RE = La, Gd, Y, Lu, Sc) compounds, J. Phys. Condens. Matter 25 (2013) 225501.
[25] P. Dorenbos, A.H. Krumpel, E. van der Kolk, P. Boutinaud, E. Cavalli, Lanthanide level location in transition metal complex compounds, Opt. Mater 32 (2010) 1681–1685.
[26] P. Dorenbos, Thermal quenching of Eu^{2+} 5d–4f luminescence in inorganic compounds, J. Phys. Condens. Matter 17 (2005) 8103–8111.
[27] F. Angiuli, E. Cavalli, A. Belletti, Synthesis and spectroscopic characterization of YPO_4 activated with Tb^{3+} and effect of Bi^{3+} co-doping on the luminescence properties, J. Solid State Chem. 192 (2012) 289–295.